International Journal of Minerals, Metallurgy and Materials
Volume 22, Number 5, May 2015, Page 537
DOI: 10.1007/s12613-015-1104-0

Surface properties of superfine alumina trihydrate after surface modification with stearic acid

Gui-hua Liu, Bo-hao Zhou, Yun-feng Li, Tian-gui Qi, and Xiao-bin Li

School of Metallurgy and Environment, Central South University, Changsha 410083, China
(Received: 19 May 2014; revised: 20 July 2014; accepted: 25 July 2014)

Abstract: The surface properties of superfine alumina trihydrate (ATH) after surface modification were studied by measuring the contact angle, active ratio, oil adsorption, total organic carbon, adsorption ratio, and Fourier transform infrared (FTIR) spectrum. The contact angle increased initially and then slowly decreased with an increase of the amount of stearic acid. However, the surface free energy decreased initially and then increased. Surface modification with stearic acid or sodium stearate can benefit from elevating temperature. The base surface tension component and the free energy of Lewis acid-base both declined sharply following the surface modification. Excess stearic acid was physically adsorbed in the form of multilayer adsorption, and an interaction between oxygen on the ATH surface and hydroxyl in stearic acid was subsequently determined. Our results further indicated that the contact angle and adsorption ratio can be used as control indicators for surface modification compared with active ratio, oil adsorption and total organic carbon.

Keywords: alumina trihydrate; surface modification; stearic acid; surface free energy; surface tension; contact angle

1. Introduction

Alumina trihydrate (ATH) is a good green filler known for its flame retardance, smoke suppressibility, and nontoxicity. However, as its hydrophilic surface results in poor interfacial compatibility and particle agglomeration in a polymeric matrix, the surface of ATH is often modified with an organic modifier [1–5]. Stearic acid (SA) is extensively employed in surface modification of ATH as it is inexpensive and remarkable efficiency. The surface properties of ATH are difficult to accurately control in surface modification since there are various interactions between SA and ATH. Therefore, it is extremely important to determine the surface properties and to understand the variation of intermolecular interactions in the ATH surface modification.

However, it remains difficult to present the surface properties accurately. Active ratio (AR) or oil adsorption is widely employed for evaluation of surface modification in China [6–10]; however, excess SA is often added in the surface modification of ATH, resulting in a loss of mechanical performance of the polymer. Fourier transform infrared (FTIR) spectrometry, scanning electron microscopy (SEM), transmission electron microscopy (TEM), and thermogravimetric analysis (TG) are not practical methods for presenting the variation of surface properties, yet they are often empolyed for improving the surface modification, discussing the surface modification mechanisms and determining the particle morphology [2–5,7,11]. Thus, it is important to reliably determine a method for evaluating the change in the surface properties accurately, based on the interaction between the modifier and the ATH surface.

Surface modification depends predominantly on the intermolecular interaction; the interaction is often classified as chemisorption (chemical adsorption) and physisorption (physical adsorption). Little research has been done on an interaction model between the functional group of stearic acid and atoms on the ATH surface. Moreover, changes in charge on the ATH surface can subsequently influence the interaction. When ATH is prepared by neutalization or hydrolysis its surface appears as a strong Lewis acid [12–14]; however, it has seldom been investigated when ATH is

Corresponding author: Bo-hao Zhou E-mail: whataboutwhat@163.com

produced by seeded precipitation from a sodium aluminate solution. In addition, the contact angle and the surface free energy can be used to determine the surface properties, however, the relations between the surface properties and surface free energy, active ratio, oil adsorption, adsorption ratio (η) or total organic carbon (TOC) remain uncertain.

In the paper, superfine ATH, prepared by seeded precipitation from a supersaturated sodium aluminate solution, was treated with stearic acid by measurements of total organic carbon, oil adsorption, active ratio, contact angle, and FTIR spectra. The surface tension and the surface free energy were subsequently calculated based on the Van Oss rule and the extended Derjguin–Landau–Verwey–Overbeek (DLVO) theory. Finally, the relationship between the macroscopic properties of ATH after surface modification (such as active ratio, the oil adsorption, total organic carbon, and adsorption ratio) and its microscopic properties (such as the free tension component, the free energy component and the intermolecular interaction) were discussed in detail. Results of this study will significantly benefit the technological development of ATH surface modification.

2. Experimental

2.1. Materials

Superfine ATH (mean particle size d_{50} = 2.59 μm) was precipitated from a supersaturated sodium aluminate solution ($\rho(Na_2O_K)=158$ g·L^{-1}, $\rho(Al_2O_3)=168$ g·L^{-1}) under conditions with an initial temperature of 60°C, a final temperature of 45°C, a precipitation time of 45 h and a superfine seed concentration of 25.16 g·L^{-1}, after which ATH was washed three times with boiling water. The mass percent of Na_2O, SiO_2, and Fe_2O_3 in superfine ATH was 0.31%, 0.026%, and 0.0091%, respectively. In addition, ATH was in the form of a hexagonal flake and (001) basal plane grows preferentially in a sodium aluminate solution, which differs from ATH by neutralization or hydrolysis.

Both stearic acid and sodium stearate (SS) were analytical grade (China National Medicines Corporation, Ltd.).

2.2. Surface modification of superfine ATH powder

ATH, stearic acid solution and deionized water were added in a flask agitated (500 r/min) in a water bath (±0.5°C). The surface modification was then carried out at 70°C–90°C for 30–60 min. The modified ATH was dried at approximately 90°C for 6–8 h after the slurry was filtered. Lastly, the contact angle, oil adsorption, active ratio, total organic carbon, and FTIR were measured after the surface modification.

2.3. Measurement

(1) The FTIR spectrum of ATH was determined by using a Nicolet 6700 spectrometer (Thermo US) with a KBr disk.

(2) The contact angle was measured with a SL200B Contact Angle Meter (Shanghai Suolun Information Technology Co., Ltd.) using the drop method with glycerin, deionized water or benzene, and the surface tension and free energy were subsequently calculated based on the Owen rule [15].

(3) The particle size distribution (PSD) was determined using a Mastersizer 2000 (Malven UK), when ATH was dispersed in deionized water.

(4) The active ratio was determined based on the standard HG/T2567. 1.0 g ATH (m_0) and 50 mL deionized water were stirred for 5 min, and the slurry was left to stand until it became clear (about 5 h). The suspended ATH was then collected, dried, and weighed as m_1. Finally, the active ratio was calculated based on the formula

$$\mathrm{AR}=\frac{m_1}{m_0}\times 100\% .$$

(5) Oil adsorption detection was carried out with castor oil at 25°C according to YS/T 618—2007 [16].

(6) Total organic carbon was determined by titration with $K_2Cr_2O_7$ according to GB 17378.5—1998 [17].

3. Results and discussion

3.1. Influence of surface modification on the contact angle

The contact angle is often used to evaluate ATH's hydrophilicity or hydrophobicity, and to calculate the surface free energy, as well as the adhesive energy. Table 1 presents the contact angle at different temperatures, with stearic acid or sodium stearate. The surface free energy and adhesive energy of ATH before and after surface modification are also listed, based on the Owen rule.

Results in Table 1 demonstrate that the contact angle increases remarkably after surface modification, and that stearic acid benefits the surface modification more than sodium stearate. This suggests that the hydrophilic surface of ATH changes and becomes partly hydrophobic after the surface modification, with the functional group in the modifier playing an important role. Moreover, an elevation in the temperature also favors surface modification with stearic acid or sodium stearate; however, in practice a higher temperature (>110°C) is not often adopted as ATH can turn into boehmite.

Table 1. Influence of surface modification on contact angle, surface free energy, and adhesive energy of superfine ATH

Type of ATH	Conditions		Surface properties		
	Modifier	Temperature / °C	Contact angle / (°)	Surface free energy / (mJ·m^{-2})	Adhesive energy / (mJ·m^{-2})
ATH	—	—	58.10	29.02	75.92
Modified ATH	SA	90	92.13	14.67	60.76
Modified ATH	SA	120	97.85	11.76	54.48
Modified ATH	SS	90	84.44	19.05	69.20
Modified ATH	SS	120	91.51	14.97	61.44

Note: Conditions of surface modification: 1% SA (SS), 20 min. Condition for measurement of contact angle: glycerin, 25°C.

Results also indicate that both the surface free energy and the adhesive energy decrease after surface modification. Stearic acid is more effective in this decrease due to its lower surface free energy and adhesive energy, implying that intermolecular interaction occurs differently in the surface modification process with stearic acid or sodium stearate at different temperatures.

3.2. Influence of surface modification on the surface free tension and energy components

Changing interactions between the modifier and atoms on the ATH surface leads to different variation tendencies in the surface free energy and the adhesive energy. Moreover, as the interactions result from van der Waals force or chemical bonds (or electrostatic force), the surface tension and the surface free energy from van der Waals or acid-base interaction can be calculated on the basis of the Van Oss rule and the extended DLVO theory.

The surface tension γ consists of the Lifshitz–van der Waals (LW) surface tension component γ^{LW}, the acid (electron acceptor) surface tension component γ^+ and the base (electron donor) surface tension component γ^- [18–21]. In this paper, the contact angle between ATH and water, glycerin or benzene is adopted for the calculation of γ^{LW}, γ^+ and γ^-, according to the following equations (Eqs. (1)–(3)).

$$\gamma_L = \gamma_L^{LW} + \gamma_L^{AB} = \gamma_L^{LW} + 2\sqrt{\gamma_L^+ \gamma_L^-} \quad (1)$$

$$\gamma_S = \gamma_S^{LW} + \gamma_S^{AB} = \gamma_S^{LW} + 2\sqrt{\gamma_S^+ \gamma_S^-} \quad (2)$$

$$\left(\gamma_L^{LW} + 2\sqrt{\gamma_L^+ \gamma_L^-}\right)(1-\cos\theta) = 2\left(\sqrt{\gamma_S^{LW}\gamma_L^{LW}} + \sqrt{\gamma_S^+ \gamma_L^-} + \sqrt{\gamma_S^- \gamma_L^+}\right) \quad (3)$$

where, γ^{AB} is the acid-base surface tension component, and subscripts S and L are abbreviations for solid and liquid, respectively. Parameters of surface tension for water, glycerin and benzene are listed in Table 2. The contact angle and calculation results can be seen in Table 3.

After surface modification, the contact angle between ATH and deionized water, glycerin, or benzene each changes differently (Table 3). The contact angle increases significantly for polar deionized water or glycerin, however, decreased slightly for non-polar benzene, validating the occurrence of a hydrophilic ATH surface following surface modification.

Table 2. Surface free energy of different substances [19]

mJ·m^{-2}

Liquids	γ_L^{LW}	γ_L^-	γ_L^+	γ_L
Water	21.8	25.5	25.5	72.8
Benzene	28.86	0	0	28.86
Glycerin	34.0	57.4	3.92	64.0

Table 3. Influence of surface modification on the contact angle and surface tension of superfine ATH powder

Sample	θ_{water} / (°)	$\theta_{glycerin}$ / (°)	$\theta_{benzene}$ / (°)	γ_S^{LW} / (mJ·m^{-2})	γ_S^- / (mJ·m^{-2})	γ_S^+ / (mJ·m^{-2})	γ_S / (mJ·m^{-2})
ATH	48.73	58.1	16.34	27.71	40.34	0.55	37.17
ATH modified with SA	111.15	92.13	14.19	27.99	0.14	0.44	28.49
ATH modified with SS	88.24	76.43	15.28	27.85	3.58	0.43	30.34

Note: Superfine ATH, addition amount 1wt%, mass ratio of liquid to solid 5, temperature 90°C, time 30 min.

Calculation results in Table 3 reveal that the Lewis base is dominant as the base surface tension component γ^- (40.34 mJ·m^{-2}) is much greater than γ^{LW} (27.71 mJ·m^{-2}) and γ^+ (0.55 mJ·m^{-2}). The Lewis base (electron donor) is assigned to oxygen on the surface of ATH as each Al cation is octahedrally coordinated by 6 hydroxyls (–OH) and each hydroxyl coordinated by two Al cations, based on the structure of alumina trihydrate. Surplus –OH remains on the surface of ATH, since there is an interface. In addition, oxygen located in the (001) basal plane of ATH has also been de-

monstrated by Gan *et al.* [22].

Moreover, different tendencies for the surface free tension component can be observed after the surface modification. Firstly, the γ_S^- (electron donor) falls sharply after surface modification, implying that oxygen on the surface of ATH "reacts" with carboxyl (–COOH) in stearic acid or carboxylate ($–COO^-$) in sodium stearate after hydrolysis. The physical adsorption of stearic acid occurs as follows, based on the change of γ_S^-:

$$(HO)_2–Al–HO^{\delta-} + H^{\delta+}OCO–R \rightarrow$$

$$(HO)_2–Al–HO^{\delta-} \cdots H^{\delta+}OCO–R \quad (4)$$

where δ^+ and δ^- represent a part positive charge and a part negative charge, respectively.

Compared with the physical adsorption, the chemical adsorption resulting from the formation of new bond is as follows:

$$(HO)_2–Al–HO^{\delta-} \cdots H^{\delta+}OCO–R \rightarrow$$

$$(HO)_2–Al–OCO–R + H_2O \quad (5)$$

In order to confirm the adsorption of stearic acid in the surface modification process, the FTIR spectra of ATH, stearic acid, and modified ATH are displayed in Fig. 1.

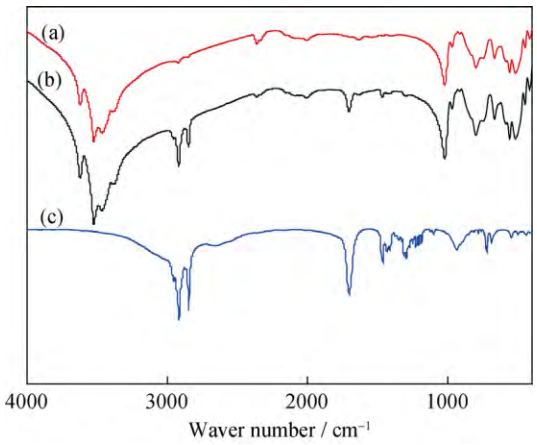

Fig. 1. FTIR spectra of alumina trihydrate (a), alumina trihydrate modified with stearic acid (b) and stearic acid (c). Surface modification under conditions: 2wt% stearic acid, 90°C, 20 min.

Peaks at 2919 cm^{-1} and 2850.13 cm^{-1} in modified ATH (Fig. 1) are assigned to the C–H bond stretching vibrations of methyl and methane, respectively, and the adsorption of C=O (carbonyl) stretching vibration is also observed at around 1706 cm^{-1}. Relative to the spectrum of stearic acid, no remarkable shift is found in the spectrum of modified ATH as only a minor amount of aluminum stearate is formed. Thus, overwhelming stearic acid is adsorbed preferentially in physical adsorption by molecular interaction, according to Eq. (4).

Secondly, results in Table 3 also show that γ^{LW} and γ^+ remain practically constant after surface modification, suggesting that the force of the van der Waals and Lewis acid (electron acceptor) change only slightly in the surface modification.

Thirdly, variation of γ^- (40.34 – 0.14 = 40.2 $mJ·m^{-2}$) for ATH modified with stearic acid is more than that of γ^- (40.34 – 3.58 = 36.76 $mJ·m^{-2}$) with sodium stearate, implying that oxygen in (001) basal plane "reacts" preferentially with the hydroxyl group –OH of stearic acid, due to the part positive charge in hydrogen atom of –OH.

In addition, the surface modification begins with the collision between the ATH particle and stearic acid, as such the distance between the modifier and the ATH particle also influences the interaction. Therefore, the effect of distance on the free energy of Lifshitz–van der Waals (ΔG_{SW}^{LW}) and Lewis acid-base (ΔG_{SW}^{AB}) can be calculated based on the extended DLVO theory [23–24].

If d (nm) is the distance between the surface of particle and the water molecule, and liquid is considered as the infinite board, the relationship between the free energy of interaction and the distance can be presented as the following equations (Eqs. (6)–(8)).

$$\Delta G_{SW}(d) = \Delta G^{LW}(d) + \Delta G^{AB}(d) \quad (6)$$

$$\Delta G_{SW}^{LW}(d) = -4\pi R\sqrt{\gamma_S^{LW}\gamma_W^{LW}}\left(\frac{d_0}{d}\right)^2 \quad (7)$$

$$\Delta G_{SW}^{AB}(d) = -4\pi R h_0\left(\sqrt{\gamma_S^+\gamma_W^-} + \sqrt{\gamma_S^-\gamma_W^+}\right)\exp\left(\frac{d_0 - d}{h_0}\right)^2 \quad (8)$$

where d_0 is the least equilibrium distance between the particle surface and the water, d_0 = (0.158 ± 0.08) nm, and h_0 = 10 nm. Water parameters are γ_W^{LW} = 21.8 $mJ·m^{-2}$, γ_W^+ = 25.5 $mJ·m^{-2}$, and γ_W^- = 25.5 $mJ·m^{-2}$.

The calculation results are shown in Table 4 and Fig. 2.

The negative ΔG_{SW}^{LW} (in Table 4) and ΔG_{SW}^{AB} (in Fig. 2) are a consequence of the attractive force.

Table 4. Influence of modifier on ΔG_{SW}^{LW} at different distances (d) 10^{-14} $mJ·m^{-2}$

Type of ATH	d / nm					
	0.5	1	3	5	7	9
Original ATH	−3.81	−1.91	−0.64	−0.38	−0.27	−0.21
ATH modified with SA	−3.87	−1.94	−0.65	−0.39	−0.28	−0.22
ATH modified with SS	−3.86	−1.93	−0.64	−0.39	−0.28	−0.21

The free energy ΔG_{SW}^{LW} and ΔG_{SW}^{AB} (Table 4 and Fig. 2) change differently in surface modification. Firstly, no significant change of ΔG_{SW}^{LW} is observed (Table 4) after surface modification, implying that the interaction from Lifshitz–van der Waals is not influenced significantly by the surface modification process. Secondly, ΔG_{SW}^{LW} is substantially less than ΔG_{SW}^{AB} for the superfine ATH, as interaction from van der Waals forces is extremely weak in comparison with the force from Lewis acid-base. For example, when d is 1 nm, ΔG_{SW}^{LW} and ΔG_{SW}^{AB} were -1.91×10^{-14} mJ·m^{-2} and -1.03×10^{-11} mJ·m^{-2}, respectively. Thirdly, both ΔG_{SW}^{LW} and ΔG_{SW}^{AB} decrease with d because the attractive force (energy) is in inverse proportion to distance. Finally, ΔG_{SW}^{AB} for stearic acid decreases remarkably following the surface modification in comparison with sodium stearate. For example, when d = 1 nm, ΔG_{SW}^{AB} for stearic acid and sodium stearate decrease 85.37% and 64.08%, respectively.

3.3. Relationship of active ratio, oil adsorption, total organic carbon, adsorption ratio, and surface free energy

The variation in macroscopic properties of ATH, such as active ratio and oil adsorption, is extensively used to this present surface modification; however, the relationship between the macroscopic properties and the surface free energy is rarely discussed. In addition, parameters of stearic acid, such as adsorption ratio and total organic carbon, are also important in surface modification. Table 5 presents the active ratio, oil adsorption, contact angle and free energy.

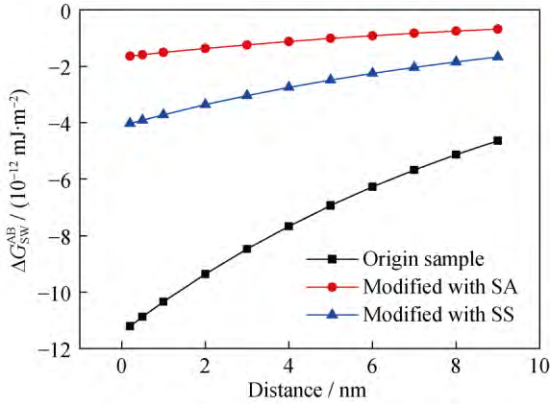

Fig. 2. Influence of distance on ΔG_{SW}^{AB}.

Table 5. Influence of the amount of stearic acid on the modified ATH

SA addition / wt%	TOC of ATH / wt%	η_{SA} / wt%	AR / wt%	Oil absorption / mL per 100 g ATH	Contact angle / (°)	Surface free energy / (mJ·m^{-2})
0	0.03	–	0	42.05	48.73	51.42
0.25	0.16	84.0	72.61	39.10	77.98	26.65
0.50	0.36	94.0	98.42	37.08	111.15	7.76
1.00	0.70	91.0	99.60	36.10	123.43	3.73
3.00	1.73	75.0	99.60	34.60	118.93	4.89
5.00	2.26	59.0	99.40	32.80	105.86	9.30

Note: adsorption ratio of SA (η_{SA}) = amount of SA in ATH / the total amount of SA × 100%; mass ratio of liquid to ATH 2, temperature 90°C, time 20 min; the contact angle is measured with deionized water.

Total organic carbon and stearic acid content in ATH increase with an increase in the amount of stearic acid (Table 5), with no "surface saturation" for stearic acid observed in the range of 0–5% stearic acid addition. However, the adsorption ratio of stearic acid (η_{SA}) increases initially and then sharply decreases with stearic acid amount, owing to the multilayer adsorption by weak van der Waals, after which a surplus stearic acid occurs. Therefore, it is important to determine which parameter (such as active ratio, oil adsorption, contact angle, adsorption ratio and total organic carbon) is sensitive to the changing surface properties, based on the relationship between the parameters and the surface free energy.

Firstly, the active ratio (Table 5) initially increases rapidly at 0–0.50% stearic acid and practically remains constant at 1.0%–5.0% stearic acid. Oil adsorption always declines with an increase in stearic acid, while the surface free energy decreases remarkably and then increases slightly with stearic acid. So variations in the active ratio and oil adsorption, as well as the total organic carbon are not in agreement with changes in the surface free energy.

Secondly, the contact angle initially increases sharply and then slowly droppes with an increase in the amount of stearic acid. Based on the calculation of surface free tension and multilayer adsorption, adsorption of surplus stearic acid on the ATH surface is likely to occur as follows:

$$(HO)_2\text{–Al–}HO^{\delta-}\cdots H^{\delta+}OCO\text{–R} + \text{R–COOH} \rightarrow (HO)_2\text{–Al–}HO^{\delta-}\cdots H^{\delta+}OCO\text{–R}\cdots ROC\text{–}OH^{\delta+} \quad (9)$$

Thus, hydrophilic –OH in the outermost layer of ATH decreases the contact angle after surface modification.

Finally, the contact angle and adsorption ratio, rather than active ratio, oil adsorption, and total organic carbon, are sensitive to the changing surface properties in surface modi-

fication, with the change of adsorption ratio also consistent with that of the free energy. Therefore, the contact angle and adsorption ratio can be employed as a control indicator for surface modification.

4. Conclusions

(1) With an increase of the amount of stearic acid in the surface modification, the total organic carbon, adsorption ratio, oil adsorption, active ratio, contact angle, and surface free energy all change differently. Adopting stearic acid or elevating temperature can benefit the surface modification of superfine ATH.

(2) γ^- and ΔG_{SW}^{AB} decrease sharply after surface modification, while γ^{LW}, γ^+ and ΔG_{SW}^{LW} all change slightly. The physical adsorption of stearic acid subsequently inferred that –OH in stearic acid interacts with oxygen on the surface of ATH, and surplus stearic acid exists when excess stearic acid is added.

(3) Contact angle and adsorption ratio are sensitive to changes in surface properties following surface modification, in comparison with active ratio, oil adsorption and total organic carbon.

Acknowledgements

This work was financially supported by the National Natural Science Foundation of China (No. 51274242).

References

[1] D.J. Kind and T.R. Hull, A review of candidate fire retardants for polyisoprene, *Polym. Degrad. Stab.*, 97(2012), No. 3, p. 201.

[2] M.A. Cárdenas, D. García-López, I. Gobernado-Mitre, J.C. Merino, J.M. Pastor, J. de D. Martínez, J. Barbeta, and D. Calveras, Mechanical and fire retardant properties of EVA/clay/ATH nanocomposites : effect of particle size and surface treatment of ATH filler, *Polym. Degrad. Stab.*, 93(2008), No. 11, p. 2032.

[3] Z.Y. Wang, F. Guo, and J.F. Chen, Surface modification of nano-aluminium trihydrate (ATH) and its flame-retardant application with ethylene-vinyl acetate (EVA), *J. Beijing Univ. Chem. Technol.*, 33(2006), No. 4, p. 9.

[4] X.Y. Zhou, C.L. Li, D.W. Huo, J. Li, and S.Y. Wu, Thermal stability and oil absorption of aluminum hydroxide treated by dry modification with different modifiers, *Trans. Nonferrous Metal. Soc. China*, 18(2008), No. 4, p. 908.

[5] W.G. Cui, Y.L. Gao, Q. Wei, and W. Mu, Influence of the surface modification of a filler on the properties of high-impact polystyrene composites, *J. Appl. Polym. Sci.*, 112(2009), No. 1, p. 359.

[6] S. Zhao, Q. Ma, B. Yu, and H. Li, Surface modification and evaluation of ultrafine $Al(OH)_3$ powder, *J. Shenyang Jianzhu Univ. Nat. Sci.*, 24(2008), No. 6, p. 1025.

[7] W.X. Hu and Z.Q. Zhang, Study on preparation and modification of nanosized aluminium hydroxide, *J. Wuhan Inst. Technol.*, 29(2007), No. 2, p. 31.

[8] S.J. Liu, W.G. Zhang, and S.L. Lei, Study on in situ combined chemical modification on surfaces of aluminum hydroxide powder, *China Plast.*, 19(2005), No. 4, p. 49.

[9] L.J. Liu, F. Guo, and J.F. Chen, Surface modification of nanosized aluminium trihydrate, *J. Beijing Univ. Chem. Technol.*, 31(2004), No. 3, p. 22.

[10] Y.N. Qin, B.L. Wu, and Y. Ni, Surface modification and thermal decomposition action of aluminum hydroxide, *J. Guilin Univ. Technol.*, 27(2007), No. 1, p. 118.

[11] X.G. Zhang, F. Guo, J.F. Chen, G.Q. Wang, and H. Liu, Investigation of interfacial modification for flame retardant ethylene vinyl acetate copolymer/alumina trihydrate nanocomposites, *Polym. Degrad. Stab.*, 87(2005), No. 3, p. 411.

[12] J.T. Trawczyński, Effect of aluminum hydroxide precipitation conditions on the alumina surface acidity, *Ind. Eng. Chem. Res.*, 35(1996), No. 1, p. 241.

[13] K. Fukushi, K. Tsukimura, and H. Yamada, Surface acidity of amorphous aluminum hydroxide, *Acta Geol. Sin.*, 80(2006), No. 2, p. 206.

[14] R. Vidruk, M.V. Landau, M. Herskowitz, V. Ezersky, and A. Goldbourt, Control of surface acidity and catalytic activity of γ-Al_2O_3 by adjusting the nanocrystalline contact interface, *J. Catal.*, 282(2011), No. 1, p. 215.

[15] D.K. Owens and R.C. Wendt, Estimation of the surface free energy of polymers, *J. Appl. Polym. Sci.*, 13(1969), No. 8, p. 1741.

[16] YS/T 618—2007 *Test Methods for Oil Adsorption of Aluminium Hydroxide for Filler*, National Development and Reform Commission of China, 2007

[17] GB 17378.5—1998, *The Specification for Marine Monitoring*: *Part* 5. *Sediment Analysis*, Standardization Administration of China, 1998

[18] C.J. van Oss, M.K. Chaudhury, and R.J. Good, The mechanism of partition in aqueous media, *Sep. Sci. Technol.*, 22(1987), No. 6, p. 1515.

[19] C.J. van Oss, R.J. Good, and R.J. Busscher, Estimation of the polar surface tension parameters of glycerol and formamide, for use in contact angle measurements on polar solids, *J. Dispersion Sci. Technol.*, 11(1990), No. 1, p. 75.

[20] H. Wang, G.H. Gu, and G.Z. Qiu, Evaluation of surface free energy of polymers by contact angle goniometry, *J. Cent. South Univ. Sci. Technol.*, 37(2006), No. 5, p. 942.

[21] Y.C. Yang, S.B. Jeong, S.Y. Yang, Y.B. Chae, and H.S. Kim, The changes in surface properties of the calcite powder with stearic acid treatment, *Mater. Trans.*, 50(2009), No. 3, p. 695.

[22] Y. Gan and G.V. Franks, Charging behavior of the gibbsite basal (001) surface in NaCl solution investigated by AFM colloidal probe technique, *Langmuir*, 22(2006), No. 14, p. 6087.

[23] H. Wang and G.H. Gu, Surface free energy of solid matter and its hydrophilic/hydrophobic nature, *Chemistry*, (2009), No. 12, p. 1091.

[24] D.Y. Kwok, D. Li, and A.W. Neumann, Evaluation of the Lifshitz–van der Waals/acid-base approach to determine interfacial tensions, *Langmuir*, 10(1994), No. 4, p. 1323.